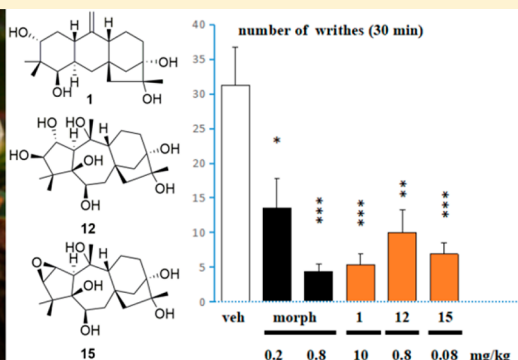


Antinociceptive Diterpenoids from the Leaves and Twigs of *Rhododendron decorum*

Yu-Xun Zhu, Zhao-Xin Zhang, Hui-Min Yan, Di Lu, Huan-Ping Zhang, Li Li, Yun-Bao Liu,^{id} and Yong Li*^{id}

State Key Laboratory of Bioactive Substance and Function of Natural Medicines, Institute of Materia Medica, Chinese Academy of Medical Sciences & Peking Union Medical College, Beijing 100050, People's Republic of China

S Supporting Information



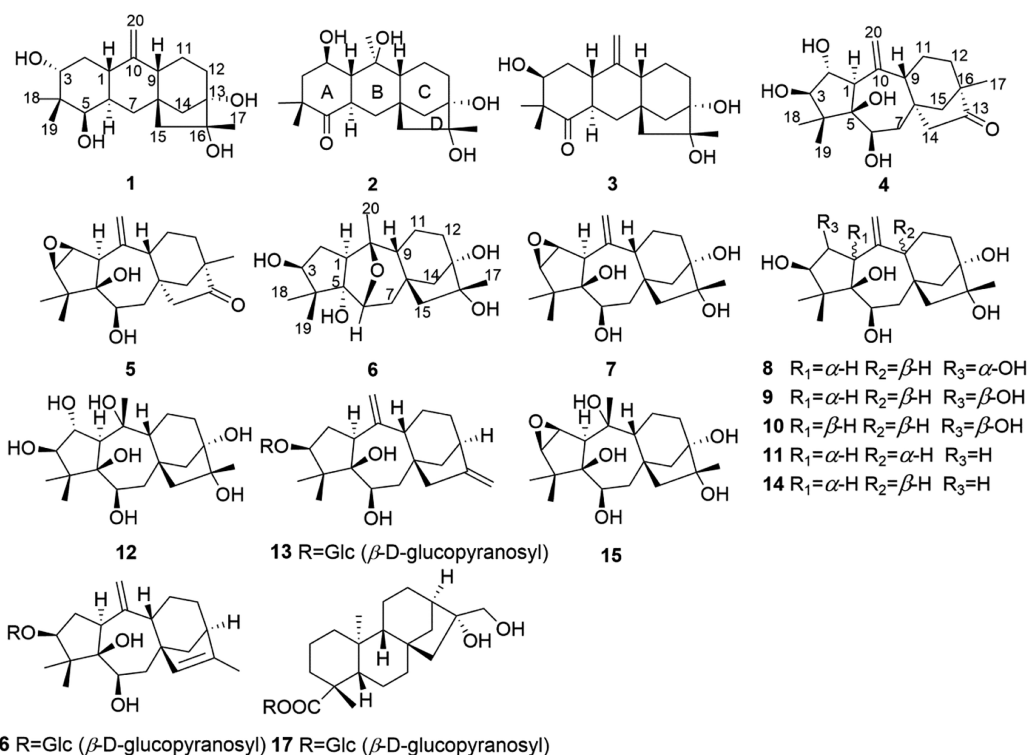
ABSTRACT: Three new leucothane-type (1–3), two new micrathane-type (4, 5), eight new grayanane-type diterpenoids (6–13), and four known compounds were obtained from the ethanol extract of the leaves and twigs of *Rhododendron decorum*. The structures were determined based on NMR spectra, quantum chemical calculations, and X-ray crystallography. The antinociceptive activities of compounds 1, 3, 4, 6, 8, 10–13, and 15–17 were evaluated via the acetic acid-induced writhing test. Compounds 1, 8, 11–13, and 15 exhibited significant antinociceptive activities. In particular, 12 and 15 were found to be effective at doses of 0.8 and 0.08 mg/kg, respectively.

Rhododendron decorum (Ericaceae) is an evergreen shrub distributed mainly in southwestern China and northeastern Burma. This plant has been used as a folk remedy for the treatment of rheumatism and pain in China for centuries.¹ However, the components of *R. decorum* have not been fully identified.^{2–5} Previous studies have shown that Ericaceae plants are rich in di- and triterpenoids.^{6–15} These compounds exhibit diverse biological activities, including antinociceptive,¹⁶ antiviral,¹⁷ sodium channel antagonistic,¹⁸ and cytotoxic effects.¹⁵ Notably, we have reported some grayanane-type diterpenoids from *Rhododendron molle* and *Pieris formosa* that have significant antinociceptive activities, and several of these compounds, such as rhodojaponin III, rhodojaponin VI, pieristoxin N, and pieristoxin P, were shown to be more potent than morphine in the acetic acid-induced writhing test.^{16,19} As a continuation of the studies on structurally unique and biologically interesting diterpenoids, an ethanol extract of the leaves and twigs of *R. decorum* was investigated and afforded 17 diterpenoids, including 13 new analogues (1–13). The isolation, structural elucidation, and antinociceptive activities of these compounds are described herein.

RESULTS AND DISCUSSION

Compound 1 was obtained as prismatic crystals. Its molecular formula was defined as C₂₀H₃₂O₄ based on high-resolution electrospray ionization mass spectrometry (HRESIMS) (*m/z* 359.2208 [M + Na]⁺, calcd 359.2193), which indicated five indices of hydrogen deficiency (IHD). The IR spectrum showed signals typical of hydroxy (3468 cm⁻¹) and olefinic (1662 cm⁻¹) functionalities. The ¹H NMR (Table 1) data showed three methyl groups (δ_{H} 1.17, 1.47, and 1.60) as well as two oxygenated methines (δ_{H} 3.52 and 4.50). The ¹³C NMR data (Table 3) and distortionless enhancement by polarization transfer (DEPT) (90°, 135°) spectrum of 1 exhibited 20 carbon resonances, including three methyls, seven methylenes, and five methines. The correlation spectroscopy (COSY) (Figure 1) and heteronuclear single-quantum correlation spectroscopy (HSQC) spectra established two fragments: CH(OH)–CH₂–CH–CH(–CH₂)–CH(OH) and CH–CH₂–CH₂. These structural features are consistent with leucothane-type diterpenoids. An exocyclic $\Delta^{10(20)}$ double bond was deduced from the signals at δ_{C} 105.4 (C-20) and 154.3 (C-10) and δ_{H} 4.96 and 5.10 (H₂-20) in conjunction with the heteronuclear

Received: November 10, 2017



multiple-bond correlation spectroscopy (HMBC) correlations from H₂-20 to C-1 (δ_c 40.7), C-9 (δ_c 49.1), and C-10 (δ_c 154.3). The HMBC correlations from H₃-18/H₃-19/H₂-2 to C-3 (δ_c 72.8), from H₂-7/H₃-18/H₃-19 to C-5 (δ_c 80.2), from H₂-14/H₃-17 to C-13 (δ_c 81.6), and from H₃-17/H₂-14 to C-16 (δ_c 77.4) placed the four hydroxy groups at C-3, C-5, C-13, and C-16, respectively. The relative configuration of **1** was deduced from its nuclear Overhauser effect spectroscopy (NOESY) spectrum. The correlations of HO-5/H-3, H-3/H-1, and H-1/H-9 indicated that HO-5, H-1, H-3, and H-9 are cofacial (β -face). The β -orientation of CH₃-17 was established via the nuclear Overhauser effect (NOE) correlations of H₃-17/H-11 β and H-15 β /H-11 β . The structure of **1** was confirmed by a single-crystal X-ray diffraction experiment (data deposited at the CCDC, no. 1580007). The X-ray crystallography data of **1** (Supporting Information) permitted its absolute configuration to be assigned as (1*S*,3*R*,5*R*,6*R*,8*R*,9*R*,13*S*,16*R*) with a Flack parameter of 0.08(13) (Figure 2). Thus, the structure of rhododecorumin I (**1**) was defined as 3 α ,5 β ,13 α ,16 α -tetrahydroxyleucoth-10(20)-ene.

Compound **2** exhibited a molecular formula of C₂₀H₃₂O₅ based on its HRESIMS data. The ¹H NMR spectrum showed resonances at δ_H 1.13, 1.14, 1.46, and 1.76 attributable to four methyl groups and a signal of an oxygenated methine at δ_H 4.70. The ¹³C NMR as well as the HSQC spectra showed signals indicative of four methyls, six methylenes, four methines (one oxygenated at δ_C 67.5), and a carbonyl group (δ_C 214.4). Based on the COSY and HMBC spectra (Figure 3), compound **2** is a leucothane-type diterpenoid. The carbonyl group was placed at C-5 via the HMBC correlations from H-6/H₃-18/H₃-19 to C-5 (δ_C 214.4). The oxygenated methine was placed at C-2 via the HMBC correlations from H-2 (δ_H 4.70) to C-1/C-3/C-4/C-6/C-10. In addition, the HMBC correlations from H₃-20 to C-1/C-9/C-10 placed a methyl group at C-10.

The NOE correlations of H₃-17/H-12 β indicated that CH₃-17 is β -oriented. The NOE correlations of H-2/H-6, H₃-20/H-2, and H₃-20/H-6 indicated that H-6, H-2, and CH₃-20 are

cofacial. However, the configuration of C-1 remains uncertain due to the lack of direct NOE evidence. The gauge including atomic orbitals (GIAO) NMR shifts of the conformers of **2** were calculated at the MPW1PW91/6-311++(2d,p) level, which has been shown to be an effective method for determining the configuration of diastereoisomers of natural products.^{20,21} From these calculations, the Bayes's theorem probability (%) of the A/B trans and A/B cis conformers were 100 and 3.4×10^{-9} (Tables S-1 and S-2, Supporting Information), respectively, which suggested a trans junction of the A/B rings in **2**. There are four possible structures (**2Aa**, **2Ab**, **2Ba**, and **2Bb**) with the A/B trans configuration (Figure 4a). Their electronic circular dichroism (ECD) spectra were calculated at the B3LYP/6-31+G(d,p) level of theory in methanol. The experimental ECD spectrum of **2** was consistent with the calculated ECD curves of **2Aa** and **2Bb**. Ultimately, the structure of **2** was assumed to be the same as **2Aa** since no natural *ent*-leucothane derivatives have been found. Thus, the structure of rhododecorumin II (**2**) was tentatively defined as 2 β ,10 β ,13 α ,16 α -tetrahydroxyleucoth-5-one.

Compound **3** was determined to have a molecular formula of C₂₀H₃₀O₄. The NMR data of **3** were similar to those of the aglycone fragment of pierisformoside F.²² Further structural analysis via 2D NMR data indicated that **3** has a hydroxy group at C-13 (δ_c 81.6). The NOE correlations of HO-3/H-1, H-1/H-9, and H-6/H₃-18 indicated that HO-3, H-1, and H-9 are β -oriented and that H-6 is α -oriented. Thus, the structure of rhododecorumin III (**3**) was defined as 3 β ,13 α ,16 α -trihydroxyleucoth-10(20)-en-5-one.

The molecular formula of **4** was defined as C₂₀H₃₀O₅, which indicated an IHD of six. The ¹H NMR data (Table 1) of **4** exhibited signals characteristic of three methyl groups (δ_H 1.02, 1.59 and 1.74), three oxygenated methine protons (δ_H 4.17, 4.29, and 4.98), and a pair of terminal olefinic protons at δ_H 5.32 and 5.55. The COSY and HSQC spectra established three fragments: CH(OH)–CH(OH)–CH, CH(OH)–CH₂, and CH–CH₂–CH₂. The 2D structural features of **4** were

Table 1. ¹H NMR Spectroscopic Data of Compounds 1–7 in Pyridine-d₅ (δ in ppm, J in Hz)

no.	1 ^a	2 ^b	3 ^b	4 ^a	5 ^b	6 ^a	7 ^b
1	2.59, t (11.8)	1.87, m	2.92, t (12.0)	3.20, d (8.0)	3.08, s	3.00, t (9.2)	3.46, brs
2	2.01, m	4.70, m	2.19, dt (13.5, 3.3)	4.98, dd (7.9, 4.0)	3.64, m	2.06, m	3.74, d (2.6)
3	2.27, dt (12.3, 3.9)		2.36, m			2.21, m	
3	4.50, m	1.91, m	4.17, m	4.17, d (3.8)	3.26, d (2.9)	4.56, dd (10.5, 6.3)	3.28, d (2.9)
4		2.22, m					
5	3.52, brd (3.8)						
6	1.91, m	2.71, td (12.2, 3.3)	2.67, td (12.1, 3.5)	4.29, brd (9.2)	3.97, d (10.6)	4.28, d (4.5)	4.06, dd (11.2, 2.9)
7	1.51, dd (12.9, 3.6)	1.73, m	1.93, d (12.2)	1.80, dd (13.6, 3.1)	1.73, dd (13.2, 3.2)	2.11, m	1.99, m
7	2.35, t (12.6)	2.17, m	2.06, m	2.42, m	2.57, dd (13.3, 11.5)	2.30, d (14.2)	2.62, t (12.2)
8							
9	2.03, m	1.74, m	1.89, m dd	2.68, dd (12.6, 4.8)	2.50, dd (12.8, 4.7)	1.89, t (8.1)	2.44, d (6.4)
10							
11	1.85, m	1.86, m	1.78, m	1.60, m	1.48, m	1.61, m	1.97, m
11	2.05, m	2.51, dd (15.3, 7.2)	1.99, dd (14.8, 6.5)	1.66, m	1.72, m	1.75, m	2.08, m
12	1.87, m	2.00, m	1.84, m	1.35, td (12.5, 6.2)	1.32, m	2.10, m	1.85, m
12	2.15, m	2.11, dd (13.4, 7.4)	2.09, m	1.42, m	1.47, m	2.12, m	2.02, m
13							
14	1.98, d (10.1)	1.98, m	1.88, m	1.62, m	1.53, m	2.46, d (11.5)	1.95, d (11.6)
14	2.19, d (9.2)	2.17, m	2.10, m	1.64, m	1.55, m	3.02, d (12.6)	2.61, d (9.8)
15	1.89, d (12.6)	1.76, m	1.81, d (14.3)	2.44, d (18.6)	2.37, d (18.3)	1.88, d (13.0)	1.89, d (15.3)
15	2.15, d (14.0)	2.21, m	2.14, d (14.1)	2.86, dd (18.3, 3.4)	2.71, dd (18.3, 3.3)	2.30, d (14.2)	2.09, d (14.2)
16							
17	1.47, s	1.46, s	1.44, s	1.02, s	1.01, s	1.52, s	1.45, s
18	1.60, s	1.14, s	1.15, s	1.59, s	1.27, s	1.45, s	1.29, s
19	1.17, s	1.13, s	1.48, s	1.74, s	1.59, s	1.41, s	1.58, s
20	4.96, s	1.76, s	4.99, s	5.32, s	5.11, s	1.32, s	5.30, s
20	5.10, s		5.10, s	5.55, s	5.52, s		5.64, s

^aRecorded at 500 MHz. ^bRecorded at 600 MHz.

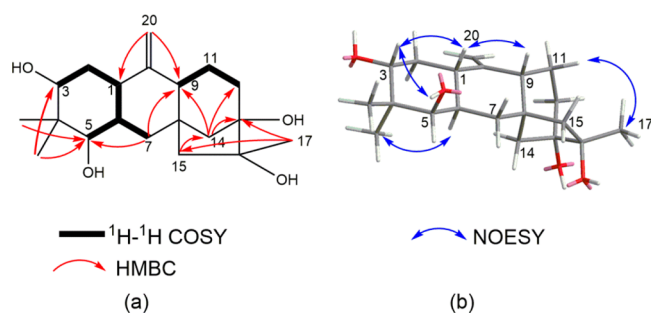


Figure 1. (a) ^1H - ^1H COSY and key HMBC correlations for **1**. (b) Selected NOESY correlations for **1**.

consistent with a grayanane diterpenoid possessing an exocyclic $\Delta^{10(20)}$ double bond. However, the correlation from H₃-17 to C-12 in the HMBC spectrum and the NOESY correlation of H-1/H-15 indicated that **4** might have a micranthane skeleton. The HMBC correlations from H-1/H-3 to C-2 suggested that, compared to micranthanone A,²³ **4** has a hydroxy group at C-2. The NOE correlations of H-3/H-1, H₃-18/H-6, H-1/H-6, and H-2/H₃-19 suggested that H-1, H-3, and H-6 are α -oriented and that H-2 is β -oriented. The NOE correlation of H-7 β /H-9 indicated that H-9 is β -oriented. Thus, the structure of rhododecorumin IV (**4**) was defined as 2 α ,3 β ,5 β ,6 β -tetrahydroxymicranthan-10(20)-en-13-one.

Compound **5**, a white solid, exhibited a molecular formula of C₂₀H₂₈O₄. The NMR data of **5** (Table 1) resembled those of **4**, except for the signals of C-2 (δ_{C} 60.0), C-3 (δ_{C} 64.8), H-2 (δ_{H} 3.64), and H-3 (δ_{H} 3.26), which indicated the presence of an epoxy moiety in **5**. According to the HMBC correlations from H-1 to C-2 and from H₃-19 to C-3, the epoxy group is located at C-2/C-3. The NOE correlations of H-1/H₃-18, H-1/H-3, and H-2/H-3 indicated that the 2,3-epoxy group is β -oriented and that H-1 and H-6 are α -oriented. Thus, the structure of rhododecorumin V (**5**) was defined as 2 β ,3 β -epoxy-5 β ,6 β -dihydroxymicranthan-10(20)-en-13-one. Compounds **4** and **5** are the second and third examples of micranthane-type diterpenoids.

Compound **6** exhibited a molecular formula of C₂₀H₃₂O₅ based on its HRESIMS data, indicating an IHD of five. Resonances attributable to six oxygenated carbons (δ_{C} 79.6, 91.1, 77.6, 84.1, 80.6, and 76.8) were observed in the ¹³C NMR data (Table 3), but the formula contains only five oxygen

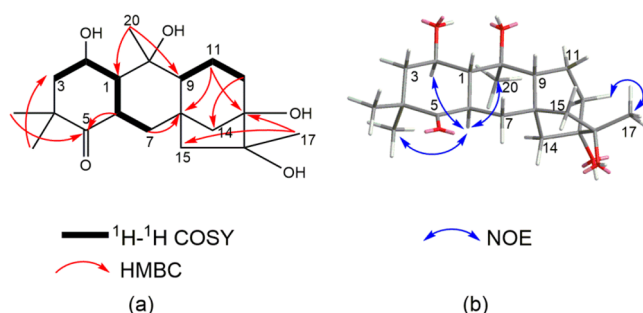


Figure 3. (a) ^1H - ^1H COSY and key HMBC correlations for **2**. (b) Selected NOE correlations for **2**.

atoms. Therefore, an oxygen bridge must be present between C-6 and C-10, which was supported by an HMBC correlation from H-6 to C-10. The NMR data of **6** were similar to those of principinaol B with two exceptions.²⁴ First, the olefinic carbons of the $\Delta^{15(16)}$ double bond in principinaol B were replaced by two sp³ carbons in **6**, which was supported by their upfield chemical shifts and the HMBC correlations from H-9 to C-15 and from H₃-17 to C-16. Second, in **6**, the hydroxy group was at C-13 instead of C-14 like it is in principinaol B, and this assignment was supported by the HMBC correlations from H₂-12 to C-14 and from H₃-17 to C-13. Thus, the structure of rhododecorumin VI (**6**) was defined as 6 β ,10 β -epoxy-3 β ,5 α ,6 α ,13 α ,16 α -pentahydroxygrayanane.

The molecular formula of **7** was determined to be C₂₀H₃₀O₅. The NMR data of **7** (Tables 1 and 3) resembled those of craibiotoxin IX (**15**).²⁵ The only difference was the dehydration at C-10 of **15** to form an exocyclic $\Delta^{10(20)}$ double bond in **7**; this assignment was made based on the deshielded chemical shifts of C-10 (**15**, δ_{C} 83.6; **7**, δ_{C} 151.3) and C-20 (**15**, δ_{C} 31.3; **7**, δ_{C} 115.9), and from the HMBC correlations from H₂-20 to C-1/C-9/C-10. Thus, the structure of rhododecorumin VII (**7**) was defined as 2 β ,3 β -epoxy-5 β ,6 β ,13 α ,16 α -tetrahydroxygrayanan-10(20)-ene.

The HRESIMS data of **8**, **9**, and **10** suggested they have the same molecular formula (C₂₀H₃₂O₆). The NMR data (Tables 2 and 3) showed that **8**, **9**, and **10** also share the same 2D structure, which was similar to that of the known diterpenoid, pieristoxin S (**14**).¹⁹ The only difference was that **8**, **9**, and **10** all possess a hydroxy substituent at C-2. For **8** and **9**, the NOE correlations of H-1/H₃-18 and H-1/H-6 suggested that H-1

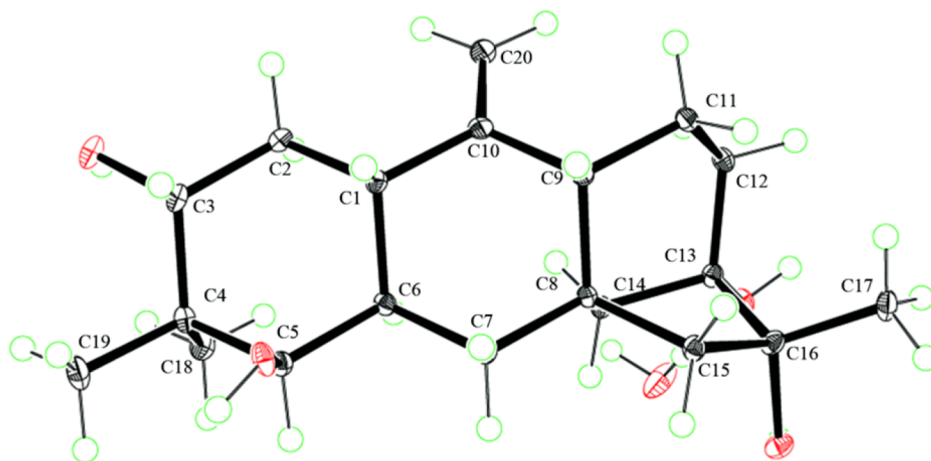


Figure 2. ORTEP drawing of **1**.

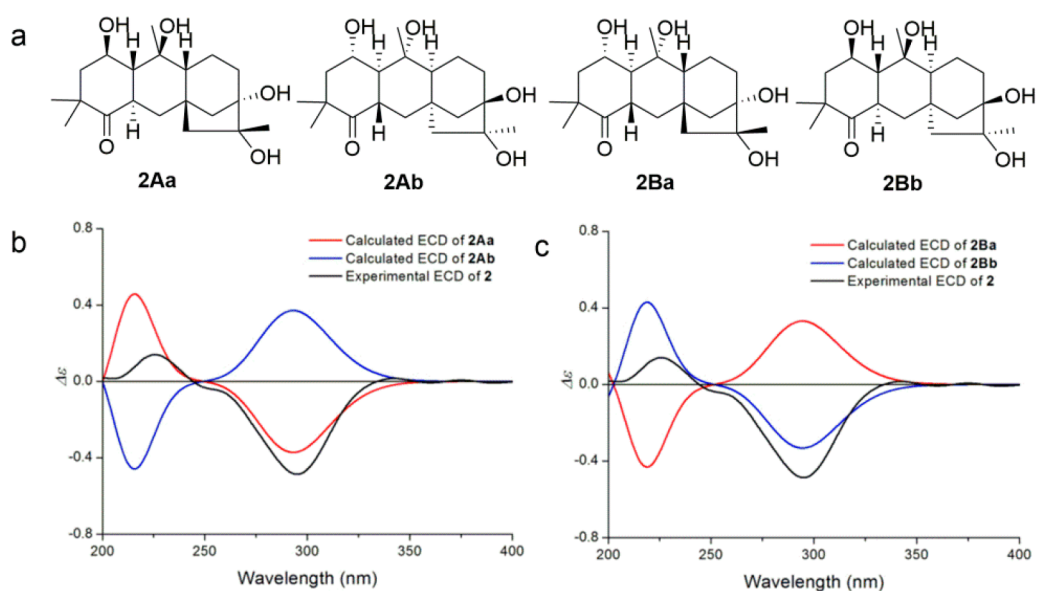


Figure 4. (a) Structures of isomers **2Aa**, **2Ab**, **2Ba**, and **2Bb**. (b) Calculated ECD spectra of **2Aa** and **2Ab** and the experimental ECD spectrum of **2**. (c) Calculated ECD spectra of **2Ba** and **2Bb** and the experimental ECD spectrum of **2**.

Table 2. ^1H NMR Spectroscopic Data of Compounds **8–13** in Pyridine- d_5 (δ in ppm, J in Hz)

no.	8^b	9^b	10^b	11^a	12^b	13^b
1	3.33, d (7.9)	2.93, d (3.4)	3.19, d (7.8)	3.25, t (9.2)	2.95, d (8.0)	2.85, dd (11.3, 7.8)
2	4.96, dd (7.7, 1.9)	4.68, brs	4.98, dd (7.8, 4.4)	2.22, m	5.19, brs	2.38, m
3	4.16, brs	4.01, d (4.8)	4.00, d (3.9)	2.40, m	4.11, brs	2.63, m
4				4.06, d (3.1)		4.21, t (6.4)
5						
6	4.36, d (7.7)	4.25, brs	3.99, d (10.7)	4.02, d (10.1)	4.33, m	4.12, m
7	1.95, brd (14.1)	1.92, d (14.0)	1.88, d (13.7)	1.88, d (13.8)	2.28, brd (13.8)	1.59, m
	2.51, t (11.5)	2.62, dd (13.4, 9.3)	3.23, dd (13.7, 10.4)	3.22, dd (13.8, 10.2)	2.65, m	2.60, m
8						
9	2.97, brs	3.06, brs	2.19, d (7.2)	2.18, d (7.8)	1.98, brd (6.8)	2.49, dd (9.0, 5.9)
10						
11	1.83, td (11.2, 4.5)	1.85, m	1.83, m	1.84, m	1.81, m	1.46, m
	2.19, m	2.05, m	1.88, m	1.94, m	2.43, dd (13.8, 6.4)	1.59, m
12	2.00, m	1.95, m	1.95, m	1.98, m	1.93, m	1.46, m
	2.20, m	2.22, m	2.21, m	2.20, m	2.90, m	1.92, m
13						
14	2.13, d (10.6)	2.04, d (10.3)	2.25, d (10.9)	2.20, d (12.0)	2.57, d (9.9)	1.27, m
	2.47, d (10.6)	2.42, d (10.5)	2.39, d (10.6)	2.39, d (9.7)	2.64, d (9.5)	1.89, d (13.1)
15	2.16, m	2.19, d (15.2)	1.78, d (14.4)	1.83, d (13.9)	2.14, brs	2.11, d (16.3)
	2.35, d (14.4)	2.34, d (14.5)	2.11, d (14.2)	2.14, d (14.3)	2.14, brs	2.35, d (15.3)
16						
17	1.50, s	1.48, s	1.40, s	1.44, s	1.50, s	4.84, s
						4.97, s
18	1.43, s	1.29, s	1.24, s	1.20, s	1.62, s	1.38, s
19	1.58, s	1.57, s	1.76, s	1.73, s	1.64, s	1.85, s
20	5.35, s	5.48, s	5.38, s	5.29, s	1.94, s	5.02, s
	5.73, s	5.80, s	5.56, s	5.31, s		5.12, s
1'						5.02, m
2'						4.06, brs
3'						4.28, m
4'						4.28, m
5'						4.44, m
6'						4.44, m
						4.60, d (11.4)

^aRecorded at 500 MHz. ^bRecorded at 600 MHz.

Table 3. ^{13}C NMR Spectroscopic Data of Compounds 1–13 in Pyridine- d_5 (δ in ppm)

no.	1 ^a	2 ^b	3 ^b	4 ^a	5 ^b	6 ^a	7 ^a	8 ^b	9 ^b	10 ^b	11 ^a	12 ^b	13 ^b
1	40.7	59.3	43.1	52.9	47.6	50.2	49.8	53.9	48.1	68.4	59.4	58.3	43.3
2	35.6	67.5	32.3	80.8	60.0	34.9	60.1	84.6	77.2	74.5	37.3	81.4	38.2
3	72.8	49.3	77.0	88.4	64.8	79.6	65.5	89.3	81.0	84.9	84.1	87.4	89.2
4	41.9	45.1	49.9	48.8	47.8	49.1	48.0	48.7	49.3	49.1	51.4	49.6	51.1
5	80.2	214.4	214.5	83.8	80.3	91.1	80.6	84.2	84.4	86.9	87.3	84.0	82.8
6	41.8	43.3	48.3	72.5	73.5	77.6	74.0	70.6	70.0	71.5	71.5	73.6	72.3
7	43.5	40.6	39.3	45.8	46.3	41.3	48.9	47.7	47.5	49.3	49.5	51.0	45.7
8	43.4	40.7	42.1	39.6	39.7	37.2	41.1	41.4	41.0	42.5	42.5	42.8	44.1
9	49.1	53.4	48.3	53.6	51.0	55.0	49.0	51.3	48.6	54.8	55.0	52.4	53.5
10	154.3	76.9	152.0	149.9	150.1	84.1	151.3	151.8	148.5	152.9	154.2	78.7	151.4
11	23.4	20.0	22.5	31.6	32.8	21.9	32.2	27.1	26.3	28.5	28.6	24.4	26.3
12	32.8	34.4	31.9	36.9	37.1	33.3	33.0	32.9	32.3	34.4	34.4	34.3	32.5
13	81.6	80.9	80.9	49.7	49.1	80.6	81.0	80.8	80.3	81.3	81.3	82.2	41.9
14	43.1	43.4	42.1	55.6	55.7	47.0	44.5	43.6	42.9	42.4	42.2	42.6	37.4
15	53.9	56.3	53.0	48.0	47.6	62.3	59.2	60.9	58.7	55.5	55.6	59.6	54.0
16	77.4	76.5	76.6	219.5	220.0	76.8	77.1	78.5	77.4	77.4	77.5	77.3	158.6
17	21.9	22.1	22.0	20.5	20.5	23.2	21.7	20.0	19.8	21.6	21.5	21.8	105.1
18	26.2	26.3	24.9	27.1	21.2	23.7	21.2	26.1	27.8	22.5	23.3	26.6	27.8
19	19.5	26.5	21.0	21.3	21.1	16.9	21.1	22.8	21.6	22.1	22.1	20.8	21.0
20	105.4	21.9	105.3	115.8	115.5	23.9	115.9	113.5	115.1	110.5	111.1	30.0	113.6
1'													106.2
2'													76.1
3'													79.1
4'													72.4
5'													79.0
6'													63.4

^aRecorded at 125 MHz. ^bRecorded at 150 MHz.

and H-6 are α -oriented. However, the relative configuration of C-2 is difficult to determine in grayanoids that lack NOE correlations between H-2 and H₃-18/H₃-19 (as for **8** and **9**). To ascertain the relative configuration at C-2, the ^{13}C NMR chemical shifts of **8** and **9** were calculated with DP4 methods (Table 4). The chemical shifts of the C-2 carbons bearing the α -OH moieties were shifted downfield (δ_{calcd} 89.43) relative to the signals of the C-2 carbons bearing β -OH substituents (δ_{calcd} 76.22). This conclusion is consistent with the data published in the last 30 years (Table S-3, Supporting Information). The experimental data of **8** and **9** are consistent with the calculated values of the 2α -OH- and 2β -OH-derivatives, respectively. Thus, the structures of rhododecorumins VIII (**8**) and IX (**9**) were defined as $2\alpha,3\beta,5\beta,6\beta,13\alpha,16\alpha$ -hexahydroxygrayanan-10(20)-ene and $2\beta,3\beta,5\beta,6\beta,13\alpha,16\alpha$ -hexahydroxygrayanan-10(20)-ene, respectively.

In the NOESY spectrum of **10**, the correlations of H-3/H₃-18, H₃-18/H-6, H-2/H₃-18, and H-1/H-9 suggested that H-2, H-3, and H-6 are α -oriented and that H-1 and H-9 are β -oriented, which indicated the A/B cis configuration of **10**. Thus, the structure of rhododecorumin X (**10**) was defined as $1\text{-}epi\text{-}2\beta,3\beta,5\beta,6\beta,13\alpha,16\alpha$ -hexahydroxygrayanan-10(20)-ene.

The HRESIMS data of **11** indicated that its molecular formula is C₂₀H₃₂O₅. The 2D structure of **11** was established based on its COSY and HMBC correlations and was found to be the same as that of pieristoxin S (**14**). The NOE correlations of H-6/H-1, H-6/H₃-18, and H-1/H-9 suggested that H-6, H-1, and H-9 are α -oriented, indicating **11** has a B/C trans configuration. Thus, the structure of rhododecorumin XI (**11**) was defined as $9\text{-}epi\text{-}3\beta,5\beta,6\beta,13\alpha,16\alpha$ -pentahydroxygrayanan-10(20)-ene.

The HRESIMS data of **12** suggested a molecular formula of C₂₀H₃₄O₇. The NMR data showed that **12** is structurally similar to **8**, except that the $\Delta^{10(20)}$ olefinic carbons in **8** were replaced by a methyl carbon at δ_{C} 30.0 and an oxygenated carbon at δ_{C} 78.7 in **12**, which was supported by the HMBC correlations from H₃-20 to C-1/C-9/C-10. Thus, the structure of rhododecorumin XII (**12**) was defined as $2\alpha,3\beta,5\beta,6\beta,10\alpha,13\alpha,16\alpha$ -heptahydroxygrayanan-10(20)-ene.

Compound **13** exhibited a molecular formula of C₂₆H₄₀O₈, indicating an IHD of seven. Compound **13** is similar to 14-deoxygrayanotoxin VIII except for the glucose unit at C-3.²⁶ This finding was supported by the HMBC correlation from H-1' to C-3. The anomeric proton at H-1' (δ_{H} 5.03) showed a large coupling constant (7.6 Hz), which indicated the glucose is in the β -configuration. Acid hydrolysis and GC analysis of the sugar moiety of **13** confirmed the sugar was D-glucose. Thus, the structure of rhododeoside I (**13**) was defined as $3\beta\text{-}[(\beta\text{-D-glucopyranosyl)oxy}]\text{-}5\beta,6\beta,13\alpha,16\alpha$ -tetrahydroxygrayanan-10(20),16(17)-diene.

The four known compounds were defined as pieristoxin S (**14**),¹⁹ craiobiotoxin IX (**15**),²⁵ pieroside A (**16**),²⁷ and paniculose IV (**17**)²⁸ by comparison of their experimental and reported NMR data.

The acetic acid-induced writhing test is usually used as a sensitive model to measure acute pain.²⁹ In this test, intraperitoneal (IP) administration was used for all the compounds. As shown in Figure 5, compounds **12** and **15** showed more potent activities than the other tested compounds. Compound **15** inhibited 78.0% of the writhes when administered at a dose of 0.08 mg/kg, while **12** inhibited 68.0% of the writhes when administered at a dose of 0.8 mg/kg. In contrast, in the same assay, morphine inhibited 86% of the

Table 4. DP4 Analysis of the ^{13}C NMR Data for Compounds 8 and 9

position	^{13}C expt	^{13}C calcd		scaled shifts		corrected error		probability	
	(8)	2 α -OH	2 β -OH	2 α -OH	2 β -OH	2 α -OH	2 β -OH	2 α -OH	2 β -OH
1	53.9	53.89	48.70	51.21	50.69	2.68	-1.99	0.13	0.20
2	84.6	89.43	76.22	85.05	82.87	4.39	-6.65	0.04	0.01
3	89.3	88.83	80.45	90.23	87.79	-1.39	-7.34	0.28	0.00
4	48.7	48.85	50.31	45.48	45.24	3.36	5.07	0.09	0.03
5	84.2	86.86	86.25	84.61	82.45	2.26	3.80	0.17	0.06
6	70.6	67.34	67.95	69.62	68.19	-2.27	-0.25	0.17	0.46
7	47.7	43.01	42.90	44.38	44.19	-1.37	-1.29	0.28	0.29
8	41.4	41.93	43.97	37.44	37.59	4.49	6.38	0.04	0.01
9	51.3	42.91	42.99	48.35	47.96	-5.44	-4.97	0.02	0.03
10	151.8	160.49	156.97	159.10	153.30	1.39	3.67	0.28	0.07
11	27.1	20.80	22.59	21.68	22.60	-0.88	-0.01	0.35	0.50
12	32.9	28.41	29.86	28.07	28.68	0.34	1.19	0.44	0.31
13	80.8	78.76	79.01	80.86	78.88	-2.10	0.12	0.19	0.48
14	43.6	43.44	42.39	39.86	39.89	3.58	2.50	0.07	0.15
15	60.9	55.45	53.48	58.93	58.02	-3.48	-4.54	0.08	0.04
16	78.5	80.68	79.83	78.32	76.47	2.35	3.36	0.16	0.09
17	20	17.07	16.58	13.85	15.16	3.21	1.43	0.10	0.27
18	26.1	18.03	23.97	20.58	21.55	-2.55	2.42	0.15	0.16
19	22.8	12.64	14.08	16.94	18.09	-4.30	-4.02	0.04	0.05
20	113.5	112.65	114.26	116.90	113.16	-4.25	1.11	0.05	0.32
product of probabilities								7.13×10^{-19}	9.55×10^{-21}
Bayes's theorem probability (%)								98.7	1.3
position	^{13}C expt	^{13}C calcd		scaled shifts		corrected error		probability	
	(9)	2 α -OH	2 β -OH	2 α -OH	2 β -OH	2 α -OH	2 β -OH	2 α -OH	2 β -OH
1	48.1	53.89	48.70	46.35	45.97	7.54	2.73	0.00	0.13
2	77.2	89.43	76.22	78.98	77.24	10.45	-1.02	0.00	0.33
3	81	88.83	80.45	83.24	81.32	5.59	-0.87	0.02	0.36
4	49.3	48.85	50.31	47.70	47.26	1.15	3.05	0.31	0.11
5	84.4	86.86	86.25	87.06	84.98	-0.19	1.27	0.47	0.30
6	70	67.34	67.95	70.91	69.50	-3.56	-1.56	0.08	0.26
7	47.5	43.01	42.90	45.68	45.32	-2.67	-2.43	0.14	0.16
8	41	41.93	43.97	38.39	38.34	3.53	5.63	0.08	0.02
9	48.6	42.91	42.99	46.91	46.51	-4.01	-3.51	0.06	0.08
10	148.5	160.49	156.97	158.93	153.86	1.56	3.11	0.26	0.10
11	26.3	20.80	22.59	21.91	22.54	-1.11	0.05	0.32	0.49
12	32.3	28.41	29.86	28.64	28.99	-0.22	0.87	0.46	0.36
13	80.3	78.76	79.01	82.46	80.57	-3.70	-1.56	0.07	0.26
14	42.9	43.44	42.39	40.52	40.38	2.92	2.01	0.12	0.20
15	58.7	55.45	53.48	58.24	57.36	-2.79	-3.88	0.13	0.06
16	77.4	80.68	79.83	79.21	77.45	1.47	2.38	0.27	0.16
17	19.8	17.07	16.58	14.62	15.56	2.45	1.03	0.16	0.33
18	27.8	18.03	23.97	23.59	24.16	-5.56	-0.18	0.02	0.47
19	21.6	12.64	14.08	16.64	17.49	-4.00	-3.42	0.06	0.08
20	115.1	112.65	114.26	121.48	117.96	-8.83	-3.70	0.00	0.07
product of probabilities								1.40×10^{-24}	1.98×10^{-15}
Bayes's theorem probability (%)								7×10^{-10}	100

writes when administered at a dose of 0.8 mg/kg. Additionally, at a dose of 10 mg/kg, **1**, **8**, **11**, and **13** showed significant antinociceptive activities compared to that of the vehicle ($p < 0.01$). Compared with our previous studies,^{16,19} two new structure–activity relationships (SARs) were elucidated based on these data. First, when the C-12–C-13 bond shifted to C-16 (microthane-type compounds such as **4**), the antinociceptive activity was lower. Second, **11** and **8** showed comparable antinociceptive activities in this study. According to a previous report,¹⁶ the oxidation degree at C-2 does not affect the activity, which suggested that the change in the configuration of the B/

C rings from cis to trans (as in **11**) may have had a small effect on the antinociceptive activity.

EXPERIMENTAL SECTION

General Experimental Procedures. IR spectra were recorded on a Nicolet 5700 FT-IR spectrometer. Optical rotations were acquired via a Rudolph automatic polarimeter. HRESIMS data were acquired on an Agilent 6520 Accurate-Mass Q-TOF LC/MS spectrometer. NMR spectra were obtained on INOVA-500, Bruker AV600-III, and INOVA SX-600 spectrometers. A Shimadzu LC-6AD instrument (SPD-20A and RID-10A detectors) was used for preparative HPLC separations. Liquid chromatography was conducted via a YMC ODS column (C₁₈,

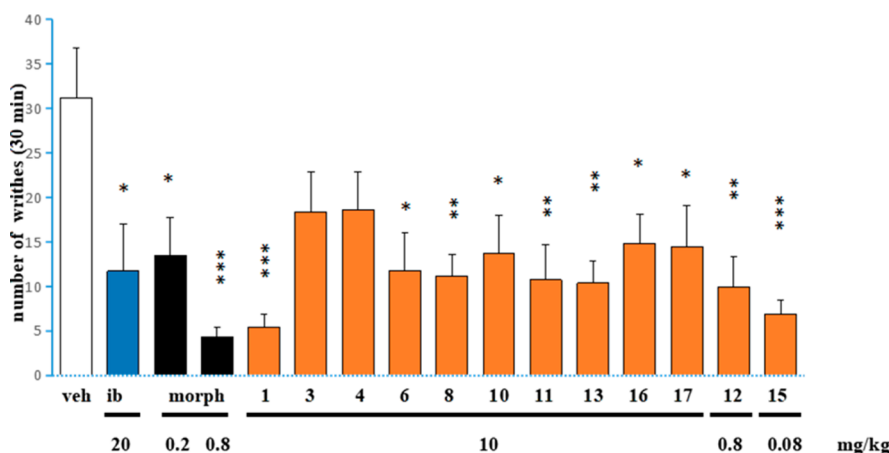


Figure 5. Antinociceptive activities of diterpenoids **1**, **3**, **4**, **6**, **8**, **10–13**, and **15–17** isolated from *R. decorum*. Data represent the mean \pm SEM * p < 0.05, ** p < 0.01, *** p < 0.001, vs vehicle (veh). Control drugs: ibuprofen (ib) and morphine (morph).

250 mm \times 20 mm, 5 μ m and C₁₈, 250 mm \times 10 mm, 5 μ m) (Kyoto, Japan). D101-type macroporous resin, Baoen Corporation (Cangzhou, China); Sephadex LH-20, GE Chemical Corporation (USA); silica gel and GF254 TLC plates, Jiangyou Corporation (Yantai, China); and ODS (50 μ m) Merck (Germany) were used for column chromatography (CC).

Plant Material. Twigs and leaves of *R. decorum* were collected in Chuxiong, Yunnan Province in April 2014. The plant was authenticated by Prof. Lin Ma of PUMC. A voucher specimen (ID-s-2603) was deposited in the herbarium of our institute.

Extraction and Isolation. Twigs and leaves of *R. decorum* (100 kg) were air-dried and extracted twice (2 h each time) with EtOH at reflux. The crude extract (not completely dry, 16 kg) was loaded into a Soxhlet extractor and extracted successively with petroleum ether, CH₂Cl₂, EtOAc, and MeOH. The EtOAc extract (1.4 kg) was separated on a macroporous resin column eluted sequentially with 70:30, 40:60, and 5:95 (v/v) H₂O–EtOH solutions. Silica gel CC was used to separate the 30% EtOH fraction (376 g). The column was eluted with a step gradient of CH₂Cl₂–MeOH (20:1, 10:1, 5:1, and 1:1, v/v). Fractions E₃₀G₁–E₃₀G₆ were collected based on the TLC results. Fraction E₃₀G₃ was separated via a Sephadex LH-20 column eluted with MeOH–H₂O (60:40, v/v) and yielded six fractions (E₃₀G₃L₁–E₃₀G₃L₆). Fraction E₃₀G₃L₁ (12.1 g) was separated via ODS column and eluted with a step gradient of MeOH/H₂O (10:90, 20:80, 30:70, 50:50, 30:70, and 100:0, v/v) to yield seven fractions, E₃₀G₃L₁M₁ to E₃₀G₃L₁M₇. Fraction E₃₀G₃L₁M₆ was separated via preparative HPLC (MeOH–H₂O, 42:58, v/v, 5 mL/min) and yielded eight fractions, E₃₀G₃L₁M₆-1 to E₃₀G₃L₁M₆-8. Fraction M₆-3 was purified via semipreparative HPLC (MeCN–H₂O, 14:86, v/v, 3.5 mL/min) to afford **4** (73.9 mg, t_R = 28.8 min). Fraction M₆-4 was purified with MeCN–H₂O (13:87, v/v, 3.5 mL/min) to afford **2** (1.2 mg, t_R = 47.9 min) and **6** (5.2 mg, t_R = 36.9 min). Fraction M₆-5 was purified with MeCN–H₂O (13:87, v/v, 3.5 mL/min) to yield **1** (11.3 mg, t_R = 26.6 min) and **14** (303.1 mg, t_R = 37.9 min). Compound **11** (11.9 mg, t_R = 17.6 min) was isolated from fraction M₆-8 using MeCN–H₂O (15:85, v/v, 3.5 mL/min). Compound **7** (4.9 mg, t_R = 23.0 min) was obtained from E₃₀G₃L₁M₇ with MeCN–H₂O (14:86, v/v, 3.5 mL/min). Fraction E₃₀G₄ was separated via Sephadex LH-20 column and yielded two fractions (E₃₀G₄L₁ and E₃₀G₄L₂). Fraction E₃₀G₄L₁ (24.1 g) was separated via an ODS column and eluted with a gradient of MeOH–H₂O (30:70, 50:50, 40:60, 30:70, 20:80, and 100:0, v/v) to yield 6 fractions, E₃₀G₄L₁M₁ to E₃₀G₄L₁M₆. Compounds **8** (7.0 mg, t_R = 7.6 min), **9** (3.2 mg, t_R = 3.2 mg, t_R = 17.3 min), and **12** (1.2 mg, t_R = 12.3 min) were isolated from E₃₀G₄L₁M₃ using HPLC with MeCN–H₂O (14:86, v/v, 3.5 mL/min). Compound **10** (6.5 mg, t_R = 8.6 min) was isolated from E₃₀G₄L₁M₂ via HPLC (MeCN–H₂O, 14:86, v/v, 3.5 mL/min). Compounds **5** (1.9 mg, t_R = 64.8 min) and **16** (9.2 mg, t_R = 52.5 min) were obtained from E₃₀G₄L₁M₆ via preparative HPLC (MeCN–H₂O, 37:63, v/v, 3.5 mL/min). The 60% EtOH fraction of

the macroporous resin column was also loaded on a silica gel column and eluted with a step gradient of CH₂Cl₂–MeOH (100:1, 40:1, 20:1, 10:1, and 5:1, v/v). Fractions G₁–G₈ were collected based on the results of TLC analysis. Fraction E₆₀G₆ was purified via Sephadex LH-20 column to yield two fractions, E₆₀G₆L₁ and E₆₀G₆L₂. Then, E₆₀G₆L₁ was purified via preparative HPLC to afford eight fractions, E₆₀G₆L₁-1 to E₆₀G₆L₁-8. E₆₀G₆L₁-2 was purified via HPLC (MeCN–H₂O, 20:80, v/v) to afford **15** (1.5 mg, t_R = 22.2 min). Compound **3** (3.6 mg, t_R = 26.2 min) was isolated from E₆₀G₆L₁-6 using preparative HPLC (MeCN–H₂O, 23:77, v/v). Fraction E₆₀G₇ was purified on a Sephadex LH-20 column to yield two fractions, E₆₀G₇L₁ and E₆₀G₇L₂. Fraction E₆₀G₇L₁ was separated via ODS into two fractions, E₆₀G₇L₁M₁ and E₆₀G₇L₁M₂. Compounds **13** (5.5 mg, t_R = 35.6 min) and **17** (1.5 mg, t_R = 13.6 min) were isolated from E₆₀G₇L₁M₂ via preparative HPLC with MeCN–H₂O (30:70, v/v, 3.5 mL/min).

Rhododecorumin I (1). [α]_D²⁰ –27 (c 0.03, MeOH); IR ν_{\max} 3468, 3244, 2935, 1662, 1446, 1408, 1087, 1040, 899 cm⁻¹; ¹H and ¹³C NMR data, see Tables 1 and 3; HRESIMS m/z 359.2208 [M + Na]⁺ (calcd for C₂₀H₃₂NaO₄, 359.2193).

Rhododecorumin II (2). [α]_D²⁰ –40 (c 0.03, MeOH); IR ν_{\max} 3384, 2927, 1702, 1659, 1452, 1374, 1090, 1056, 1032, 858 cm⁻¹; ¹H and ¹³C NMR data, see Tables 1 and 3; HRESIMS m/z 375.2156 [M + Na]⁺ (calcd for C₂₀H₃₂NaO₅, 375.2142).

Rhododecorumin III (3). [α]_D²⁰ –29 (c 0.1, MeOH); IR ν_{\max} 3472, 2938, 1699, 1644, 1445, 1391, 1065, 1039, 938, 912 cm⁻¹; ¹H and ¹³C NMR data, see Tables 1 and 3; HRESIMS m/z 357.2038 [M + Na]⁺ (calcd for C₂₀H₃₀NaO₄, 357.2036).

Rhododecorumin IV (4). [α]_D²⁰ –44 (c 0.2, MeOH); IR ν_{\max} 3410, 2928, 1731, 1630, 1455, 1404, 1075, 1042, 805 cm⁻¹; ¹H and ¹³C NMR data, see Tables 1 and 3; HRESIMS m/z 373.1988 [M + Na]⁺ (calcd for C₂₀H₃₀NaO₅, 373.1985).

Rhododecorumin V (5). [α]_D²⁰ –73 (c 0.03, MeOH); IR ν_{\max} 3416, 2930, 1732, 1598, 1465, 1379, 1363, 1205, 1123, 1088, 851 cm⁻¹; ¹H and ¹³C NMR data, see Tables 1 and 3; HRESIMS m/z 355.1884 [M + Na]⁺ (calcd for C₂₀H₂₈NaO₄, 355.1880).

Rhododecorumin VI (6). [α]_D²⁰ –60 (c 0.01, MeOH); IR ν_{\max} 3372, 2940, 1730, 1645, 1587, 1453, 1379, 1121, 1066, 1041, 951, 855 cm⁻¹; ¹H and ¹³C NMR data, see Tables 1 and 3; HRESIMS m/z 375.2140 [M + Na]⁺ (calcd for C₂₀H₃₂NaO₅, 375.2142).

Rhododecorumin VII (7). [α]_D²⁰ –90 (c 0.01, MeOH); IR ν_{\max} 3362, 2927, 1595, 1415, 1122, 1088, 1044, 857 cm⁻¹; ¹H and ¹³C NMR data, see Tables 1 and 3; HRESIMS m/z 373.1986 [M + Na]⁺ (calcd for C₂₀H₃₀NaO₅, 373.1985).

Rhododecorumin VIII (8). [α]_D²⁰ –53 (c 0.02, MeOH); IR ν_{\max} 3383, 2943, 1630, 1601, 1451, 1382, 1334, 1081, 1056, 965, 815 cm⁻¹; ¹H and ¹³C NMR data, see Tables 2 and 3; HRESIMS m/z 369.2277 [M + H]⁺ (calcd for C₂₀H₃₃O₆, 369.2272).

Rhododecorumin IX (9). [α]_D²⁰ –90 (c 0.01, MeOH); IR ν_{\max} 3364, 2942, 1677, 1450, 1384, 1336, 1082, 915, 836 cm⁻¹; ¹H and ¹³C NMR

data, see Tables 2 and 3; HRESIMS m/z 369.2274 $[M + H]^+$ (calcd for $C_{20}H_{33}O_6$, 369.2272).

Rhododecorumin X (10). $[\alpha]_D^{20}$ -2 (c 0.1, MeOH); IR ν_{max} 3415, 2942, 1675, 1637, 1450, 1385, 1336, 1078, 1040, 894 cm^{-1} ; 1H and ^{13}C NMR data, see Tables 2 and 3; HRESIMS m/z 391.2093 $[M + Na]^+$ (calcd for $C_{20}H_{32}NaO_6$, 391.2091).

Rhododecorumin XI (11). $[\alpha]_D^{20}$ $+7$ (c 0.1, MeOH); IR ν_{max} 3388, 2939, 1675, 1637, 1450, 1063, 1040, 1012, 892, 857 cm^{-1} ; 1H and ^{13}C NMR data, see Tables 2 and 3; HRESIMS m/z 375.2147 $[M + Na]^+$ (calcd for $C_{20}H_{32}NaO_5$, 375.2142).

Rhododecorumin XII (12). $[\alpha]_D^{20}$ -50 (c 0.01, MeOH); IR ν_{max} 3370, 2968, 1675, 1450, 1381, 1337, 1080, 1057, 913, 848 cm^{-1} ; 1H and ^{13}C NMR data, see Tables 2 and 3; HRESIMS m/z 409.2201 $[M + Na]^+$ (calcd for $C_{20}H_{34}NaO_7$, 409.2197).

Rhododeoside I (13). $[\alpha]_D^{20}$ -38 (c 0.1, MeOH); IR ν_{max} 3382, 2932, 1655, 1448, 1367, 1079, 1042, 878 cm^{-1} ; 1H and ^{13}C NMR data, see Tables 2 and 3; HRESIMS m/z 503.2630 $[M + Na]^+$ (calcd for $C_{26}H_{40}NaO_8$, 503.2615).

Acid Hydrolysis and GC Analysis of the Sugar Moiety of Compound 13. The configuration of the sugar moiety was established according to the published method.^{30,31} Compound 13 (1.0 mg) was dissolved in MeOH (2 mL), and the solution was added to 2 N HCl (3 mL). The solution was heated at 90 °C for 13 h. The reaction mixture was evaporated and partitioned with EtOAc and H_2O . The aqueous layer was concentrated to furnish the sugar mixture, which was dissolved in dry pyridine and reacted with L-cysteine methyl ester hydrochloride (2 mg) at 60 °C for 2 h. After removal of the solvent, N-trimethylsilylimidazole (0.5 mL) was added, and the mixture was heated at 60 °C for 2 h. The mixture was evaporated to dryness, and the residue partitioned into n-hexane and H_2O . Anhydrous Na_2SO_4 was added to the organic layer to remove residual water. The sample was analyzed on a GC system equipped with an FID (detector temperature, 300 °C). Chromatography conditions: injection temperature, 280 °C; column, HP-5 (60 m \times 0.32 mm \times 0.25 μm); initial column temperature, 200 °C; column temperature increased to 280 °C (10 °C/min) and kept at 280 °C for 35 min under N_2 carrier gas.

In the GC chromatogram, the derivatives of the acid hydrolysate of 13 and the D-glucose standard showed approximate retention times of 20.31 and 20.45 min, respectively.

Animals. Male Kunming mice (16–20 g) were housed for 3 days before use. Food and water were freely available. Animal experiments were conducted following the guidelines of the NIH, and experimental procedures were approved by the Ethics Committee of our institute. The doses administered in each test were based on preliminary experiments. The mice used to test each compound were removed from the cages at random. The behavior reaction of each mouse was independently counted by three observers to minimize subjective bias.

Acetic Acid-Induced Writhing Tests. Kunming mice (eight per group) were used in the tests. Control mice received 0.9% NaCl by intraperitoneal injection (10 mL/kg), and the test mice received aqueous solutions of the different compounds (hydrotropic agent, Tween 80) by intraperitoneal injection (10 mg/kg). 15 minutes later, 0.8% v/v HOAc solution (0.1 mL/10 g) was administered to the mice by intraperitoneal injection. The number of writhing events for each mouse was counted for 30 min.

■ ASSOCIATED CONTENT

● Supporting Information

The Supporting Information is available free of charge on the ACS Publications website at DOI: 10.1021/acs.jnatprod.7b00941.

IR, HRESIMS, 1H and ^{13}C NMR, HSQC, HMBC, and NOESY spectra of compounds 1–13 (PDF)
Crystallographic data for compound 1 (CIF)

■ AUTHOR INFORMATION

Corresponding Author

*Phone: 86-10-63165324. Fax: 86-10-83162679. E-mail: liyong@imm.ac.cn.

ORCID

Yun-Bao Liu: 0000-0002-1338-0271

Yong Li: 0000-0003-1672-6589

Notes

The authors declare no competing financial interest.

■ ACKNOWLEDGMENTS

This work was supported by grants from the National Natural Science Foundation of China (Grant Nos. 21572274 and 81630094) and the CAMS Innovation Fund for Medical Sciences (Grant No. 2016-I2M-3-012).

■ REFERENCES

- (1) Chinese Materia Medica Compilation Commission. *Chinese Materia Medica*; Shanghai Scientific & Technical Publishers: Shanghai, China, 1999; Vol. 16, p 5260.
- (2) Zhang, H. P.; Wang, H. B.; Wang, L. Q.; Bao, G. H.; Qin, G. W. *J. Asian Nat. Prod. Res.* **2005**, *7*, 87–90.
- (3) Zhang, W. D.; Jin, H. Z.; Chen, G.; Li, X. F.; Yan, S. K.; Zhang, L.; Shen, Y. H.; Yang, M. *Fitoterapia* **2008**, *79*, 602–604.
- (4) Rateb, M. E.; Hassan, H. M.; Arafa, el-SA.; Jaspars, M.; Ebel, R. *Nat. Prod. Commun.* **2014**, *9*, 473–476.
- (5) Jin, H. Z.; Chen, G.; Li, X. F.; Shen, Y. H.; Yan, S. K.; Zhang, L.; Yang, M.; Zhang, W. D. *Chem. Nat. Compd.* **2009**, *45*, 85–86.
- (6) El-Naggar, S. F.; Doskotch, R. *J. Nat. Prod.* **1980**, *43*, 617–631.
- (7) Klocke, J. A.; Hu, M. Y.; Chiu, S. F.; Kubo, I. *Phytochemistry* **1991**, *30*, 1797–1800.
- (8) Li, C. J.; Wang, L. Q.; Chen, S. C.; Qin, G. W. *J. Nat. Prod.* **2000**, *63*, 1214–1217.
- (9) Chen, S. N.; Zhang, H. P.; Wang, L. Q.; Bao, G. H.; Qin, G. W. *J. Nat. Prod.* **2004**, *67*, 1903–1906.
- (10) Zhong, G. H.; Hu, M. Y.; Wei, X. Y.; Weng, Q. F.; Xie, J. J.; Liu, J. X.; Zhang, W. X. *J. Nat. Prod.* **2005**, *68*, 924–926.
- (11) Huang, X. Z.; Wang, Y. H.; Yu, S. S.; Fu, G. M.; Hu, Y. C.; Liu, Y.; Fan, L. H. *J. Nat. Prod.* **2005**, *68*, 1646–1650.
- (12) Li, C. H.; Niu, X. M.; Luo, Q.; Xie, M. J.; Luo, S. H.; Zhou, Y. Y. *Org. Lett.* **2010**, *12*, 2426–2429.
- (13) Li, Y.; Liu, Y. B.; Yu, S. S. *Phytochem. Rev.* **2013**, *12*, 305–325.
- (14) Niu, C. S.; Li, Y.; Liu, Y. B.; Ma, S. G.; Liu, F.; Li, C.; Yu, H. B.; Wang, X. J.; Qu, J.; Yu, S. S. *Tetrahedron* **2018**, *74*, 375–382.
- (15) Lv, X. J.; Li, Y.; Ma, S. G.; Qu, J.; Liu, Y. B.; Li, Y. H.; Zhang, D.; Li, L.; Yu, S. S. *J. Nat. Prod.* **2016**, *79*, 2824–2837.
- (16) Li, Y.; Liu, Y. B.; Zhang, J. J.; Liu, Y.; Ma, S. G.; Qu, J.; Lv, H. N.; Yu, S. S. *J. Nat. Prod.* **2015**, *78*, 2887–2895.
- (17) Li, Y.; Liu, Y. B.; Zhang, J. J.; Li, Y. H.; Jiang, J. D.; Yu, S. S.; Ma, S. G.; Qu, J.; Lv, H. N. *Org. Lett.* **2013**, *15*, 3074–3077.
- (18) Li, C. J.; Liu, H.; Wang, L. Q.; Jin, M. W.; Chen, S. N.; Bao, G. H.; Qin, G. W. *Acta. Chim. Sin.* **2003**, *61*, 1153–1156.
- (19) Niu, C. S.; Li, Y.; Liu, Y. B.; Ma, S. G.; Li, L.; Qu, J.; Yu, S. S. *Tetrahedron* **2016**, *72*, 44–49.
- (20) Smith, S. G.; Goodman, J. M. *J. Am. Chem. Soc.* **2010**, *132*, 12946–12959.
- (21) Tuan, N. Q.; Oh, J.; Park, H. B.; Ferreira, D.; Choe, S. *Phytochemistry* **2017**, *133*, 45–50.
- (22) Wang, L. Q.; Chen, S. N.; Cheng, K. F.; Li, C. J.; Qin, G. W. *Phytochemistry* **2000**, *54*, 847–852.
- (23) Zhang, M. K.; Zhu, Y.; Zhan, G. Q.; Shu, P. H.; Sa, R. J.; Lei, L.; Xiang, M.; Xue, Y. B.; Luo, Z. W.; Wan, Q.; Yao, G. M.; Zhang, Y. H. *Org. Lett.* **2013**, *15*, 3094–3097.
- (24) Liu, C. C.; Lei, C.; Zhong, Y.; Gao, L. X.; Li, J. Y.; Yu, M. H.; Li, J.; Hou, A. J. *Tetrahedron* **2014**, *70*, 4317–4322.

- (25) Zhang, W. D.; Jin, H. Z.; Chen, G.; Li, X. F.; Yan, S. K.; Zhang, L.; Shen, Y. H.; Yang, M. *Fitoterapia* **2008**, *79*, 602–604.
- (26) Zhang, M. K.; Xie, Y. Y.; Zhan, G. Q.; Lei, L.; Shu, P. H.; Chen, Y. L.; Xue, Y. B.; Luo, Z. W.; Wan, Q.; Yao, G. M.; Zhang, Y. H. *Phytochemistry* **2015**, *117*, 107–115.
- (27) Wang, L. Q.; Li, C. J.; Chen, S. N.; Qin, G. W. *Chinese Traditional and Herbal Drugs* **2000**, *31*, 407–409.
- (28) Yamasaki, K.; Kohda, H.; Kobayashi, T.; Kaneda, N.; Kasai, R.; Tanaka, O.; Nishi, K. *Chem. Pharm. Bull.* **1977**, *25*, 2895–2899.
- (29) Niu, C. S.; Li, Y.; Liu, Y. B.; Ma, S. G.; Liu, F.; Li, L.; Xu, S.; Wang, X. J.; Liu, S.; Wang, R. B.; Qu, J.; Yu, S. S. *RSC Adv.* **2017**, *7*, 43921–43932.
- (30) Hara, S.; Okabe, H.; Mihashi, K. *Chem. Pharm. Bull.* **1987**, *35*, 501–506.
- (31) Feng, Z. M.; Song, S.; He, J.; Yang, Y. N.; Jiang, J. S.; Zhang, P. *C. Carbohydr. Res.* **2013**, *380*, 59–63.